

University of Nebraska - Lincoln

DigitalCommons@University of Nebraska - Lincoln

Papers in Natural Resources

Natural Resources, School of

12-1-2021

A physiological signal derived from sun-induced chlorophyll fluorescence quantifies crop physiological response to environmental stresses in the U.S. Corn Belt

Hyungsuk Kimm

University of Illinois Urbana-Champaign, hk8@illinois.edu

Kaiyu Guan

University of Illinois Urbana-Champaign, kaiyug@illinois.edu

Chongya Jiang

University of Illinois Urbana-Champaign

Guofang Miao

University of Illinois Urbana-Champaign

Genghong Wu

University of Illinois Urbana-Champaign

Follow this and additional works at: <https://digitalcommons.unl.edu/natrespapers>

See next page for additional authors



Part of the [Natural Resources and Conservation Commons](#), [Natural Resources Management and Policy Commons](#), and the [Other Environmental Sciences Commons](#)

Kimm, Hyungsuk; Guan, Kaiyu; Jiang, Chongya; Miao, Guofang; Wu, Genghong; Suyker, Andrew; Ainsworth, Elizabeth A.; Bernacchi, Carl J.; Montes, Christopher M.; Berry, Joseph A.; Yang, Xi; Frankenberg, Christian; Chen, Min; and Köhler, Philipp, "A physiological signal derived from sun-induced chlorophyll fluorescence quantifies crop physiological response to environmental stresses in the U.S. Corn Belt" (2021). *Papers in Natural Resources*. 1529.

<https://digitalcommons.unl.edu/natrespapers/1529>

This Article is brought to you for free and open access by the Natural Resources, School of at DigitalCommons@University of Nebraska - Lincoln. It has been accepted for inclusion in Papers in Natural Resources by an authorized administrator of DigitalCommons@University of Nebraska - Lincoln.

Authors

Hyungsuk Kimm, Kaiyu Guan, Chongya Jiang, Guofang Miao, Genghong Wu, Andrew Suyker, Elizabeth A. Ainsworth, Carl J. Bernacchi, Christopher M. Montes, Joseph A. Berry, Xi Yang, Christian Frankenberg, Min Chen, and Philipp Köhler

LETTER • OPEN ACCESS

A physiological signal derived from sun-induced chlorophyll fluorescence quantifies crop physiological response to environmental stresses in the U.S. Corn Belt

To cite this article: Hyungsuk Kimm *et al* 2021 *Environ. Res. Lett.* **16** 124051

View the [article online](#) for updates and enhancements.

You may also like

- [Exposure to cold temperature affects the spring phenology of Alaskan deciduous vegetation types](#)
Mingjie Shi, Nicholas C Parazoo, Su-Jong Jeong *et al.*
- [Land cover change alters seasonal photosynthetic activity and transpiration of Amazon forest and Cerrado](#)
Maria del Rosario Uribe and Jeffrey S Dukes
- [Kenyan tea is made with heat and water: how will climate change influence its yield?](#)
A J Rigden, V Ongoma and P Huybers

ENVIRONMENTAL RESEARCH
LETTERS

LETTER

OPEN ACCESS

RECEIVED
15 September 2021REVISED
24 October 2021ACCEPTED FOR PUBLICATION
18 November 2021PUBLISHED
6 December 2021

Original content from
this work may be used
under the terms of the
[Creative Commons
Attribution 4.0 licence](#).

Any further distribution
of this work must
maintain attribution to
the author(s) and the title
of the work, journal
citation and DOI.

A physiological signal derived from sun-induced chlorophyll
fluorescence quantifies crop physiological response
to environmental stresses in the U.S. Corn BeltHyungsuk Kimm^{1,2,*} , Kaiyu Guan^{1,2,3,*} , Chongya Jiang^{1,2} , Guofang Miao² , Genghong Wu^{1,2} ,
Andrew E Suyker⁴ , Elizabeth A Ainsworth^{5,6} , Carl J Bernacchi^{5,6} , Christopher M Montes⁶ ,
Joseph A Berry⁷ , Xi Yang⁸ , Christian Frankenberg^{9,10} , Min Chen^{11,12} and Philipp Köhler⁹

- ¹ Agroecosystem Sustainability Center, Institute for Sustainability, Energy, and Environment, University of Illinois Urbana-Champaign, Urbana, IL, 61801, United States of America
 - ² Department of Natural Resources and Environmental Sciences, College of Agricultural, Consumers, and Environmental Sciences, University of Illinois Urbana-Champaign, Urbana, IL, 61801, United States of America
 - ³ National Center for Supercomputing Applications, University of Illinois Urbana-Champaign, Urbana, IL, 61801, United States of America
 - ⁴ School of Natural Resources, University of Nebraska, Lincoln, NE 68583, United States of America
 - ⁵ Department of Plant Biology, University of Illinois Urbana-Champaign, Urbana, IL, 61801, United States of America
 - ⁶ USDA-ARS, Global Change and Photosynthesis Research Unit, Urbana, IL 61801, United States of America
 - ⁷ Department of Global Ecology, Carnegie Institution for Science, Stanford, CA 94305, United States of America
 - ⁸ Department of Environmental Sciences, University of Virginia, Charlottesville, VA 22903, United States of America
 - ⁹ Division of Geological and Planetary Sciences, California Institute of Technology, Pasadena, CA, United States of America
 - ¹⁰ Jet Propulsion Laboratory, California Institute of Technology, Pasadena, CA, United States of America
 - ¹¹ Department of Forest and Wildlife Ecology, University of Wisconsin-Madison, Madison, WI, United States of America
 - ¹² Nelson Institute Center for Climatic Research, University of Wisconsin-Madison, Madison, WI, United States of America
- * Authors to whom any correspondence should be addressed.

E-mail: hk8@illinois.edu and kaiyug@illinois.edu**Keywords:** sun-induced chlorophyll fluorescence, U.S. Corn Belt, T-FACE, corn and soybean, physiological stress, physiological SIF yield, TROPOMI**Abstract**

Sun-induced chlorophyll fluorescence (SIF) measurements have shown unique potential for quantifying plant physiological stress. However, recent investigations found canopy structure and radiation largely control SIF, and physiological relevance of SIF remains yet to be fully understood. This study aims to evaluate whether the SIF-derived physiological signal improves quantification of crop responses to environmental stresses, by analyzing data at three different spatial scales within the U.S. Corn Belt, i.e. experiment plot, field, and regional scales, where ground-based portable, stationary and space-borne hyperspectral sensing systems are used, respectively. We found that, when controlling for variations in incoming radiation and canopy structure, crop SIF signals can be decomposed into non-physiological (i.e. canopy structure and radiation, 60% ~ 82%) and physiological information (i.e. physiological SIF yield, Φ_F , 17% ~ 31%), which confirms the contribution of physiological variation to SIF. We further evaluated whether Φ_F indicated plant responses under high-temperature and high vapor pressure deficit (VPD) stresses. The plot-scale data showed that Φ_F responded to the proxy for physiological stress (partial correlation coefficient, $r_p = 0.40$, $p < 0.001$) while non-physiological signals of SIF did not respond ($p > 0.1$). The field-scale Φ_F data showed water deficit stress from the comparison between irrigated and rainfed fields, and Φ_F was positively correlated with canopy-scale stomatal conductance, a reliable indicator of plant physiological condition (correlation coefficient $r = 0.60$ and 0.56 for an irrigated and rainfed sites, respectively). The regional-scale data showed Φ_F was more strongly correlated spatially with air temperature and VPD ($r = 0.23$ and 0.39) than SIF ($r = 0.11$ and 0.34) for the U.S. Corn Belt. The lines of evidence suggested that Φ_F reflects crop physiological responses

to environmental stresses with greater sensitivity to stress factors than SIF, and the stress quantification capability of Φ_F is spatially scalable. Utilizing Φ_F for physiological investigations will contribute to improve our understanding of vegetation responses to high-temperature and high-VPD stresses.

1. Introduction

Crop remote sensing needs to quantify environmental stress impacts on both canopy structure and plant physiology to fully understand environmental impacts on crop productivity and yield (Hatfield *et al* 2008, Guan *et al* 2017). Although remote sensing-based monitoring has been effective in quantifying crop responses to various environmental stresses, it has been primarily focused on the structural variability of crops and insufficient in quantifying physiological stress impacts. Commonly used remote sensing-based approaches are the estimation of leaf area index (LAI) or canopy chlorophyll content, both of which are an effective predictor of crop growth and crop yield, and vegetation indices are developed and tested to better estimate those variables (Viña *et al* 2011, Lobell *et al* 2015, Cai *et al* 2019, Kimm *et al* 2020b). However, existing approaches are unable to quantify immediate non-structural stress impacts, i.e. physiological down-regulation such as depressions in instantaneous photosynthetic rate, reproductive, and carbon-allocation processes (Erdle *et al* 2013, Hatfield and Prueger 2015, Fleta-Soriano and Munné-Bosch 2016, Guan *et al* 2016, 2017). To understand environmental impacts on crops better, it is necessary to make a distinction between structural and physiological impacts and to quantify them separately.

Remote sensing-based quantification of plant physiology has been relatively limited, but new opportunities became available with the advances of sun-induced chlorophyll fluorescence (SIF) measurements. SIF has shown its potential for quantifying plant physiological variability through higher accuracy and sensitivity in quantifying crop productivity or crop stress when compared to existing remote sensing approaches (Sun *et al* 2015, Song *et al* 2018, Li *et al* 2020a). A SIF signal includes information on both plant physiological variation and canopy structural variation. Structural information of SIF has been relatively well understood. Initially, plant canopy-absorbed radiation (absorbed photosynthetically active radiation, APAR) was used to explain SIF signals related to the canopy structural variability and incoming radiation (Miao *et al* 2020, Yang *et al* 2018a). More recently, near-infrared reflectance of vegetation (Badgley *et al* 2017, 2019) and near-infrared radiance of vegetation (NIRvR) (Wu *et al* 2019, Baldocchi *et al* 2020) were found to better account for structural- and radiation information, and were used to address the dominance of such non-physiological information in far-red SIF.

A physiological signal of SIF, however, has not been fully recognized so far because of the dominant contribution of canopy structural variation, a lack of physiological stress, and a relatively large magnitude of uncertainty in previous SIF datasets (Dechant *et al* 2020, 2022, Miao *et al* 2020). Following a recently introduced framework of understanding SIF signal (Dechant *et al* 2020), physiological information can be better derived through normalization of SIF by other components, i.e. incoming PAR, the fraction of chlorophyll-absorbed PAR (fAPAR), and escaping ratio (fesc) that describes the measured fraction of SIF photons that escape a plant canopy (Zeng *et al* 2019). Estimated physiological information of SIF, denoted as Φ_F , has been found to be relatively constant from continuous datasets (Dechant *et al* 2020, Liu *et al* 2020), but only few studies focused on such a physiological aspect of SIF. Considering the mechanistic link between SIF and photochemistry (Porcar-Castell *et al* 2014, van der Tol *et al* 2014), Φ_F may include useful physiological information, which is yet to be found.

Recently, there are more opportunities available for studying SIF-derived physiological information at different scales and under different circumstances as SIF data become available at various spatial scales through different platforms. Commonly used SIF platforms are ground-based (portable and stationary), air-borne, and space-borne sensing systems. Datasets from different platforms are complementary in observing spatiotemporal variation of SIF and underscore different aspects of SIF in estimating plant productivity or plant stress. A ground-based portable system usually collects data from experimental plots with specific environmental controls and evaluates the capability of SIF in quantifying plant stress responses (Helm *et al* 2020, Kimm *et al* 2021). A ground-based stationary measurement collects continuous data that are often paired with other measurements such as CO₂, water, and energy fluxes from an Eddy Covariance-based flux tower. The data usually include a long-term record for biological and meteorological variables, which allow for in-depth evaluation of the observed SIF (Liu *et al* 2017, Miao *et al* 2018, 2020, Yang *et al* 2018a, Li *et al* 2020b). Airborne and space-borne measurements most efficiently collect data from large areas. These datasets quantify spatial variation over large areas, and findings from such data are spatially representative (Sun *et al* 2015, Guan *et al* 2016, Song *et al* 2018, Li *et al* 2020a). Given the complementing characteristics of different SIF datasets, to include multi-scale and multi-platform data

is critical for achieving a thorough understanding of SIF.

This study focused on the U.S. Corn Belt where one-third of the global corn and soybean supply is produced, and we investigated non-physiological and physiological information contained in far-red SIF (SIF indicates far-red SIF throughout the manuscript) responding to the major crop stress factors, high temperature and high vapor pressure deficit (VPD). Specifically, we derived non-physiological and physiological information of SIF from three different spectral datasets based on different platforms at different scales and analyzed the derived physiological SIF yield (Φ_F) to evaluate relative advantages of Φ_F signals in understanding crop response to environmental stresses. To obtain a comprehensive understanding, we used three datasets that include different sources of physiological variability, heating treatment effect, controlled water management, and a large natural gradient of temperature and VPD. The overarching question of this study is: Whether SIF-derived physiological signals help us understand and quantify the physiological impacts of high-temperature and high-VPD stresses in the U.S. Corn Belt. Specific questions are: (a) what is the relative importance of the non-physiological signal vs. plant physiological signal in SIF variability under different environmental variabilities? (b) Do the SIF-derived physiological signals indicate plant responses to high-temperature and high-VPD stress and contribute to quantifying physiological stress impacts? If so, to what extent? This study will address the potential improvement of crop monitoring by disaggregating SIF signals into non-physiological and physiological signals and by evaluating the derived physiological signals. Explicit consideration of physiological responses of crops will allow for comprehensive assessment and understanding of crop growth and its interaction with the surrounding environment.

2. Materials and methods

2.1. Data

Data was collected from three platforms at different temporal and spatial scales (table 1). The plot-scale dataset was collected by a ground-based portable system in a warming experiment for soybean (Kimm *et al* 2021). The field-scale dataset was collected by ground-based stationary systems at adjacent irrigated and rainfed corn-soybean rotation fields. The regional-scale dataset was collected by MODIS and TROPOMI space-borne platforms covering the U.S. Corn Belt.

2.1.1. Plot-scale data

The warming experiment was conducted in 2019 at the SoyFACE facility located in Champaign, Illinois (40°02'30.5" N 88°13'58.8" W). The experiment included an ambient level and four treatment levels

of canopy temperature (+1.5 °C, +3.0 °C, +4.5 °C, and +6.0 °C) with two replicates. Infrared heaters were used to warm the canopy temperature to a set point and to achieve specific increments compared to the ambient plot. Real-time canopy temperature measurements were made using a thermal infrared radiometer in each plot. Further details can be found in (Kimm *et al* 2021). Spectral measurements were made using a portable system prepared for rapid data collection over the 12 plots (an ambient plot per two treatment plots where the total 8 treatment plots were designed with 4 levels of treatment and 2 replicates). The system included a low spectral resolution, wide spectral range spectrometer and a high spectral resolution (0.15 nm full width at half maximum, i.e., full width at half maximum (FWHM), and spectral range from 630 to 800 nm), narrow spectral range spectrometer (1.10 nm FWHM and spectral range from 350 to 1100 nm) to collect spectral reflectance for visible and near-infrared waveband and SIF retrieval.

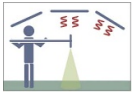
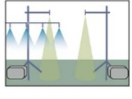
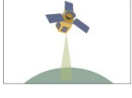
2.1.2. Field-scale data

The stationary observation sites of this study are two corn-soybean rotation fields in Saunders, NE (41°10'46.8" N 96°26'22.7" W and 41°09'53.5" N 96°28'12.4" W). A combined spectral measurement system, the Fluospec2 system, was deployed at the two sites on a 5 m height scaffold (Miao *et al* 2018, Yang *et al* 2018b). Similar to plot-scale data collection, Fluospec2 included two spectrometers with different specifications, and collected spectral data at two different spectral range and resolution (See Miao *et al* (2018) for the instrumentation details, and see Miao *et al* (2020) for the data collection details). The data were collected in 2017 and 2018, but 2018 was an abnormally wet year (no water deficit stress) and thus was out of the scope of this study. The spectral measurements were collected next to eddy covariance flux towers registered at AmeriFlux network (site IDs are US-Ne2 and US-Ne3, <https://ameriflux.lbl.gov/>), and we also used water flux and meteorology data from these flux towers for part of our analysis.

2.1.3. Regional-scale data

We used SIF retrieval from TROPOMI data (Köhler *et al* 2018), surface reflectance for red and near-infrared waveband of MODIS, and incident photosynthetically active radiation (PAR) derived by applying machine learning methods to MODIS land and atmospheric products (Jiang *et al* 2020a). Additionally, we used daily maximum temperature and daily maximum VPD of PRISM climate data (<https://prism.oregonstate.edu/>) to analyze a relationship between climatic variables and SIF signals, crop data layer (CDL) from National Agricultural Statistics Service of United States Department of Agriculture (USDA) to focus on croplands, and irrigation map data to confirm the scope to the rainfed areas.

Table 1. Description of the datasets used in this study.

	Platform	Target	Stress	Spatial scale (footprint)	Temporal scale	Reference
	Ground-based portable system	Warming experiment plots	Temperature	<1 m radius	Daily (discrete)	Kimm <i>et al</i> (2021)
	Ground-based stationary systems	Irrigated vs rainfed crop fields	VPD	<5 m radius	Half-hourly (continuous)	Miao <i>et al</i> (2020)
	Space-borne system	U.S. Corn Belt	Temperature and VPD	$0.05^\circ \times 0.05^\circ$	Daily (continuous)	Köhler <i>et al</i> (2018)

Daily frequency TROPOMI SIF data were collected with a footprint scale of 3.5 km by 7 km at nadir view (Köhler *et al* 2018) and were resampled at 0.05° resolution for comparisons with gridded datasets, and cloudy pixels were excluded from the analysis. TROPOMI SIF retrieval algorithm was thoroughly tested in an earlier study (Köhler *et al* 2018), and the quantified retrieval model error was <1% of measured radiance ($\sim 200 \text{ mW m}^{-2} \text{ sr}^{-1} \text{ nm}^{-1}$) but could be more than 20% for the retrieved SIF due to its small magnitude ($\sim 3 \text{ mW m}^{-2} \text{ sr}^{-1} \text{ nm}^{-1}$). To minimize the uncertainty for SIF as well as Φ_F calculation (see section 2.2 for Φ_F derivation), the data at 0.05° were aggregated at 0.25° of spatial resolution. For consistency with the SIF data, daily 250 m-resolution MODIS surface reflectance and 1 km-resolution PAR data were prepared in the same way. These MODIS data were first aggregated within each footprint of SIF data and then resampled at 0.05° grid. In this study, we only assessed corn and soybean that are the most common commodities in the U.S. Corn Belt by selecting only the pixels with greater than 60% of the combined fraction of corn and soybean based on CDL land cover type data. The land cover data were also similarly prepared as SIF data by calculating the fraction of corn and soybean at each pixel of the aggregated 0.05° grid. To minimize the potential impact of irrigation in evaluating climatic impacts on crops, irrigated areas were excluded from the analysis (the fraction of irrigated area >10%) based on the irrigation map data from Xie *et al* (2019).

2.2. SIF disaggregation

We applied an advanced framework for interpreting a SIF signal (Dechant *et al* 2020, Zeng *et al* 2020), which disaggregates it into non-physiological and physiological signals. Following thorough testing based on simulations, we used either NIRvP or soil-adjusted NIRvP (SANIRvP) as a proxy for non-physiological (i.e. canopy structure and radiation) signals included in SIF, and they are obtained as follows:

$$\text{NDVI} = (\rho_{\text{NIR}} - \rho_{\text{Red}}) / (\rho_{\text{NIR}} + \rho_{\text{Red}}) \quad (1)$$

$$\text{NIRv} = \rho_{\text{NIR}} \cdot \text{NDVI} \quad (2)$$

$$\text{NIRvP} = \text{NIRv} \cdot \text{PAR} \quad (3)$$

$$\text{SANIRvP} = \text{NIRv}_{\text{max}} \cdot \frac{\text{NIRv} - \text{NIRv}_{\text{min}}}{\text{NIRv}_{\text{max}} - \text{NIRv}_{\text{min}}} \cdot \text{PAR} \quad (4)$$

where NIRv is an approximation of near-infrared reflectance of vegetation, PAR is incident photosynthetically active radiation, and NIRvmax and NIRvmin are long-term maximum and minimum of NIRv. SANIRvP accounts for soil impact through normalizing NIRv as shown in equation (4), but as it requires long-term records for the reliable consideration of soil impact, it was only used for satellite datasets. Proximal remote sensing-derived NIRvP and satellite-based SANIRvP used different PAR units. NIRvP used instantaneous photon flux density ($\mu\text{mol photon m}^{-2} \text{ s}^{-1}$) whereas SANIRvP used daily radiation energy flux ($\text{MJ m}^{-2} \text{ d}^{-1}$) (Jiang *et al* 2020a). We then derived Φ_F using (SA)NIRvP following the below calculations:

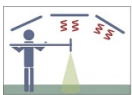
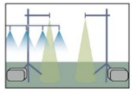

$$\text{SIF} = \text{PAR} \times f_{\text{APAR}_{\text{chl}}} \times f_{\text{esc}} \times \Phi_F \quad (5)$$

$$f_{\text{esc}} = \text{NIRv} / f_{\text{APAR}_{\text{chl}}} \quad (6)$$

$$\Phi_F = \text{SIF} / \text{NIRvP}. \quad (7)$$

The derivation of Φ_F is based on the consideration of non-physiological impacts on the canopy-scale observation of SIF that involves multiple factors, i.e. incident radiation, leaf-to-canopy scaling parameters such as LAI and leaf angle distribution. As (SA)NIRvP accounts for the photosystem-to-canopy scaling, the ratio of SIF to (SA)NIRvP allows for estimating photosystem-scale fluorescence yield, which is linked to photochemical yield and stomatal conductance (equations (3), (5)–(7)) (Zeng *et al* 2020).

Table 2. Description of data preprocessing.

Target	Spatial scale	Temporal scale	Time of day	Time of year
 Warming experiment plots	<1 m radius	Daily (discrete)	10 AM–3 PM	20 July–15 September → 20 July–4 September
 Irrigated vs rainfed crop fields	<5 m radius	Half-hourly (continuous) → Daily	9 AM–6 PM → 10 AM–2 PM	May–October → July–August
 U.S. Corn Belt	$0.25^\circ \times 0.25^\circ$	Daily (continuous)	10 AM–2 PM	January–December → Peak three week period

2.3. Data analysis

2.3.1. Data preprocessing

We preprocessed the data for our analyses to reduce variations of incoming radiation and canopy structure, which are non-physiological and directly associated with SIF, and to focus on the impacts of high temperature and high VPD on crop physiology. For the two ground-based sensing datasets, time of day and time of year are restricted to peak radiation hours and peak growth season. Particularly for the field-scale data, time of day was set corresponding to the overpass time of TROPOMI data, and the spectral data were aggregated at the daily timescale (table 2). For the TROPOMI data, we only selected the data from a three week period of the highest NIRv on a pixel basis in each year to minimize the pixel-to-pixel difference caused by different phenological stages and to focus on crop responses in their peak growth period. We obtained the three week period mean values and analyzed spatial patterns.

2.3.2. Relative importance analysis

To quantify relative importance, we calculated the relative sum of squares from analysis of variance (ANOVA), i.e. a sum of square for each term (SS_{NIRvP} , SS_{SANIRvP} or SS_{Φ_F}) divided by the total sum of square (SS_{Total}). The ANOVA was conducted to the below regression model:

$$\text{SIF} = c_1 + c_2 \cdot \text{NIRvP} + c_3 \cdot \varphi_F \quad (8)$$

where c_1 , c_2 , and c_3 are regression coefficients. To keep the consistency of our analysis across different datasets, we focused on temporal variability rather than spatial variability. ANOVA was conducted for each plot, each site, and each pixel, respectively, and then we averaged the quantified relative importance across different plots, sites, and pixels and obtained a 95% confidence interval from their variability (figures 2(a) and (c)).

2.3.3. Plot-scale data

We used simple linear regression and partial correlation analysis to evaluate to what extent NIRvP and Φ_F

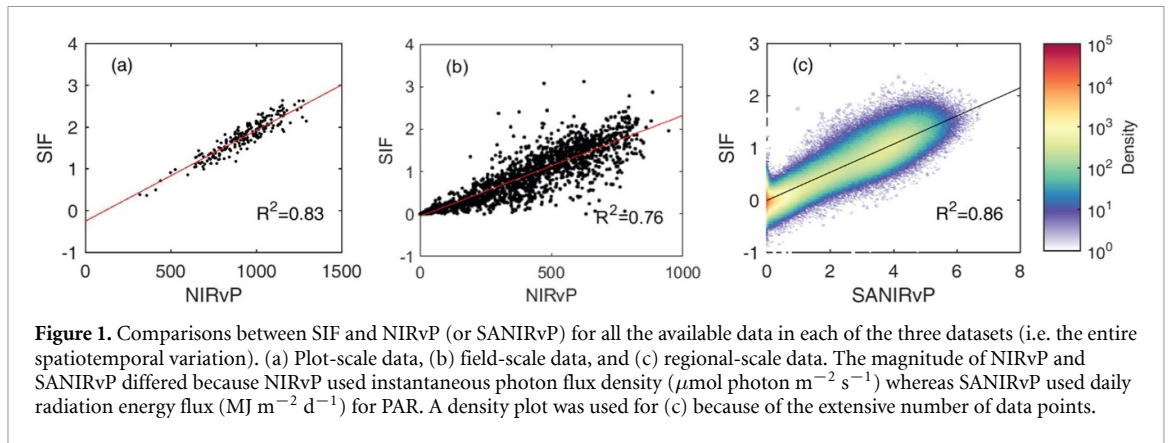
were associated with non-physiological and physiological stress. We used green chlorophyll vegetation index (GCVI), which is developed for estimating leaf- and canopy-scale chlorophyll content (Gitelson *et al* 2005), as a proxy for canopy structure. Since the plot-scale data included a manipulated gradient of canopy temperature, we approximated physiological stress by using canopy temperature. Considering the continuity of the warming treatments, structural and physiological impacts were presumed to be collinear. To account for the collinearity between variables, we used partial correlation analysis including GCVI and canopy temperature as an explanatory variable. For correlation analysis and partial correlation analysis, we reported Pearson's correlation coefficient (r and r_p , respectively).

2.3.4. Field-scale data

We first compared SIF, NIRvP, and Φ_F between the irrigated and rainfed fields and used t-test for significance test. Then further investigated whether the observed Φ_F difference indicates plant physiological difference by testing its relation with canopy stomatal conductance (G_s). G_s is regarded as a proxy for plant physiological responses, especially under water-deficit stress (Kimm *et al* 2020a, Zhang *et al* 2021) and was obtained by applying the inverted Penman-Monteith equation to the estimated evapotranspiration from Ameriflux tower data (US-Ne1 and US-Ne2, Ameriflux network), which includes minimal surface evaporation impact by removing data possibly affected by precipitation or leaf-surface dew formation. Further details can be found in Kimm *et al* (2020a).

2.3.5. Regional-scale data

We evaluated whether Φ_F potentially contributed to improving our capability of quantifying plant response to high-temperature and high-VPD stresses by analyzing the satellite data along with PRISM climate data. Here we used mean values of the selected three week period, which was the peak season, i.e. the highest mean SANIRv on a pixel basis, to minimize the phenological variability across pixels. We used



the Pearson correlation analysis to evaluate how crops in the U.S. Corn Belt responded to the variability of air temperature and VPD through the three variables, SIF, SANIRvP, and Φ_F .

3. Results

3.1. Relative importance of the disaggregated signals of SIF

We first evaluated the importance of the non-physiological information for the spatiotemporal variation of all the available SIF data in each dataset. The determination coefficient (R^2) of the relationship between SIF and (SA)NIRvP was >0.82 in the three datasets (figure 1). Less than 20% of the SIF variation was potentially attributable to plant physiological information. Considering the uncertainty of the measurements and SIF retrieval, this value maybe even less than 10%. To quantify and evaluate clearer physiological signals from SIF, we controlled temporal variations in radiation and seasonality of canopy development. Before and after the preprocessing, we disaggregated SIF into (SA)NIRv and Φ_F that represent a non-physiological and physiological signal, respectively, and quantified the relative importance of each component from the three datasets (figure 2). Although (SA)NIRvP explained the majority of SIF variability in both cases, our relative importance results showed that a physiological signal of SIF occupied a significant portion of SIF variability after the preprocessing and indicated potential applications of SIF-derived physiological signals. With all data included, the relative importance of (SA)NIRvP explained 64%–91% of SIF variability, and Φ_F explained 0%–20% (5%, 20%, and 0% for the plot-scale, field-scale, and regional-scale datasets, respectively, figure 2). After preprocessing the data, (SA)NIRvP explained less (60%–82%) and Φ_F explained more of SIF variation (28%, 31%, and 17%, respectively for the plot-scale, field-scale, and regional-scale dataset). In both cases, the plot-scale and field-scale datasets showed greater importance of Φ_F than the satellite dataset.

3.2. SIF-derived physiological signals for understanding plant responses to high-VPD and high-temperature stresses

For each of the three different datasets, we tested whether (if so, to what extent) the SIF-derived physiological signals indicate physiological stress to high-temperature and water deficit stress. First, linear regression analysis of the plot-scale dataset showed that both NIRvP and Φ_F were significantly correlated with GCVI and canopy temperature (T_c), and NIRvP-GCVI and Φ_F - T_c showed the greatest association suggesting that NIRvP and Φ_F contained information on non-physiological variation and physiological stress, respectively (correlation coefficient for NIRvP-GCVI: 0.47, NIRvP- T_c : -0.28 , Φ_F -GCVI: 0.35, and Φ_F - T_c : -0.50 , $p < 0.001$ for all cases) (figures 3(a)–(d)). In partial correlation analysis, including GCVI and canopy temperature as an explanatory variable, collinearity between the two variables was accounted for, and we evaluated more strictly whether Φ_F were indicative of physiological stress. We found from the partial correlation results that the SIF-GCVI correlation was largely attributed to NIRvP (partial correlation r_p for NIRvP-GCVI: 0.4, $p < 0.001$, and for Φ_F -GCVI: 0.16, $p > 0.01$), while the SIF-canopy temperature correlation was entirely attributed to Φ_F (r_p for Φ_F - T_c : -0.4 , $p < 0.001$, and for NIRvP- T_c : not significant, $p > 0.1$), which showed even greater sensitivity to canopy temperature than SIF ($r_p = -0.28$, $p < 0.001$) (figure 3(e)).

Second, the field-scale data included different water-deficit levels by different management practices (i.e. irrigation or rainfed). We first compared SIF, NIRvP, and Φ_F between the two fields and found a statistically significant difference only in Φ_F ($p < 0.001$), which showed an 18% relative difference (two sites' difference normalized by the value of the irrigated site) (figure 4(a)). The smaller Φ_F in the rainfed site suggested water deficit stress of the crops, and the lack of SIF difference indicates that Φ_F could have a better ability to detect stress than SIF. Further, both G_s and Φ_F showed smaller values in the rainfed site, which supported stronger stomatal regulation and photosynthetic depression caused by water

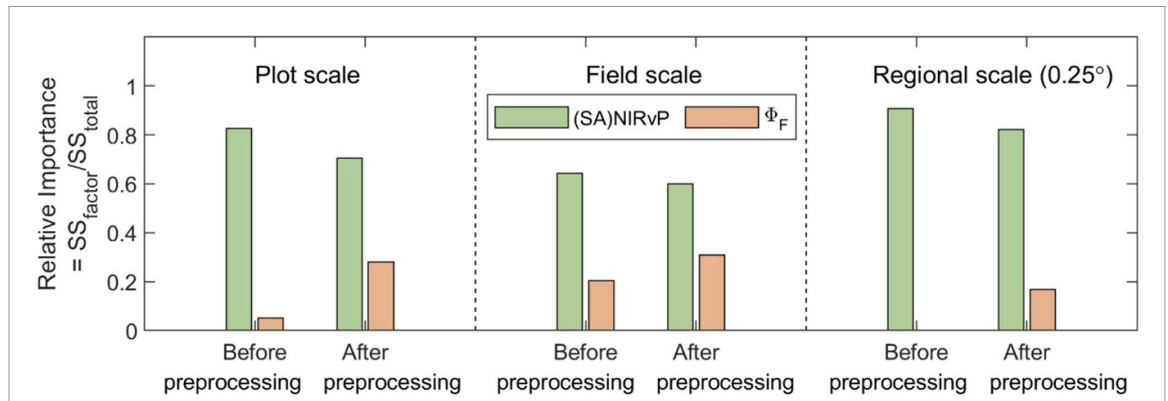


Figure 2. The relative importance of NIRvP (or SANIRvP) and Φ_F in explaining the spatiotemporal variation of SIF from the plot-scale data (a), field-scale data (b), and regional-scale data (c) before and after the data preprocessing. SS_{factor} and SS_{total} are sum of square values from ANOVA.

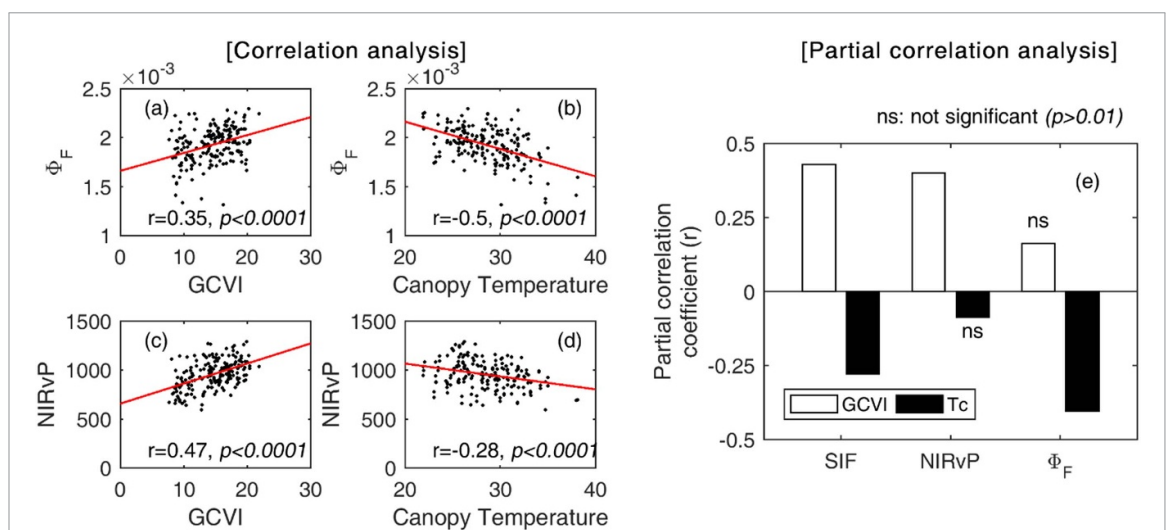


Figure 3. Left side plots show a scatter plot with a linear regression line for one-to-one relationships for Φ_F and GCVI (a), Φ_F and Tc (b), NIRvP and GCVI (c), and NIRvP and Tc (d). The right-hand side plot shows partial correlation analysis result for SIF, NIRvP, and Φ_F explained by GCVI and canopy temperature (Tc) with the consideration of collinearity (e).

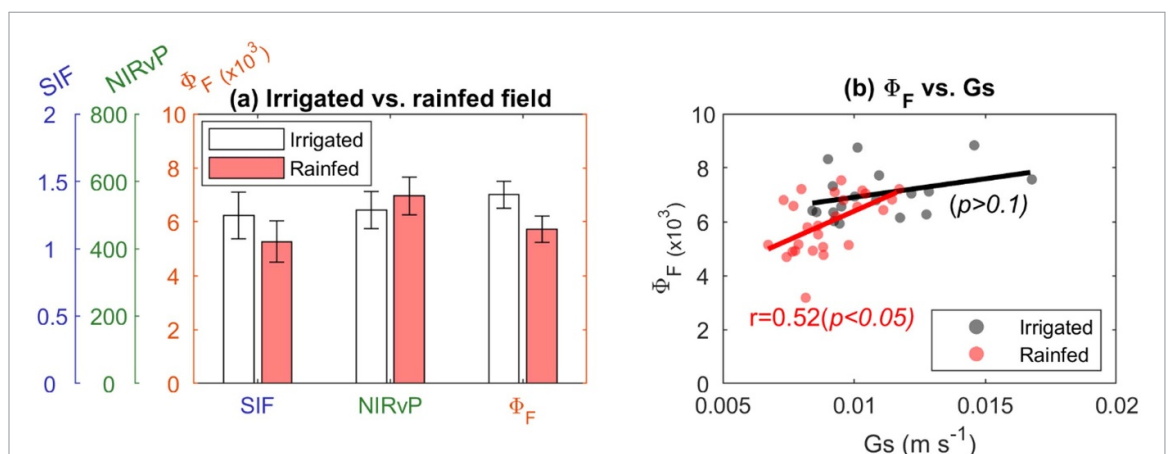
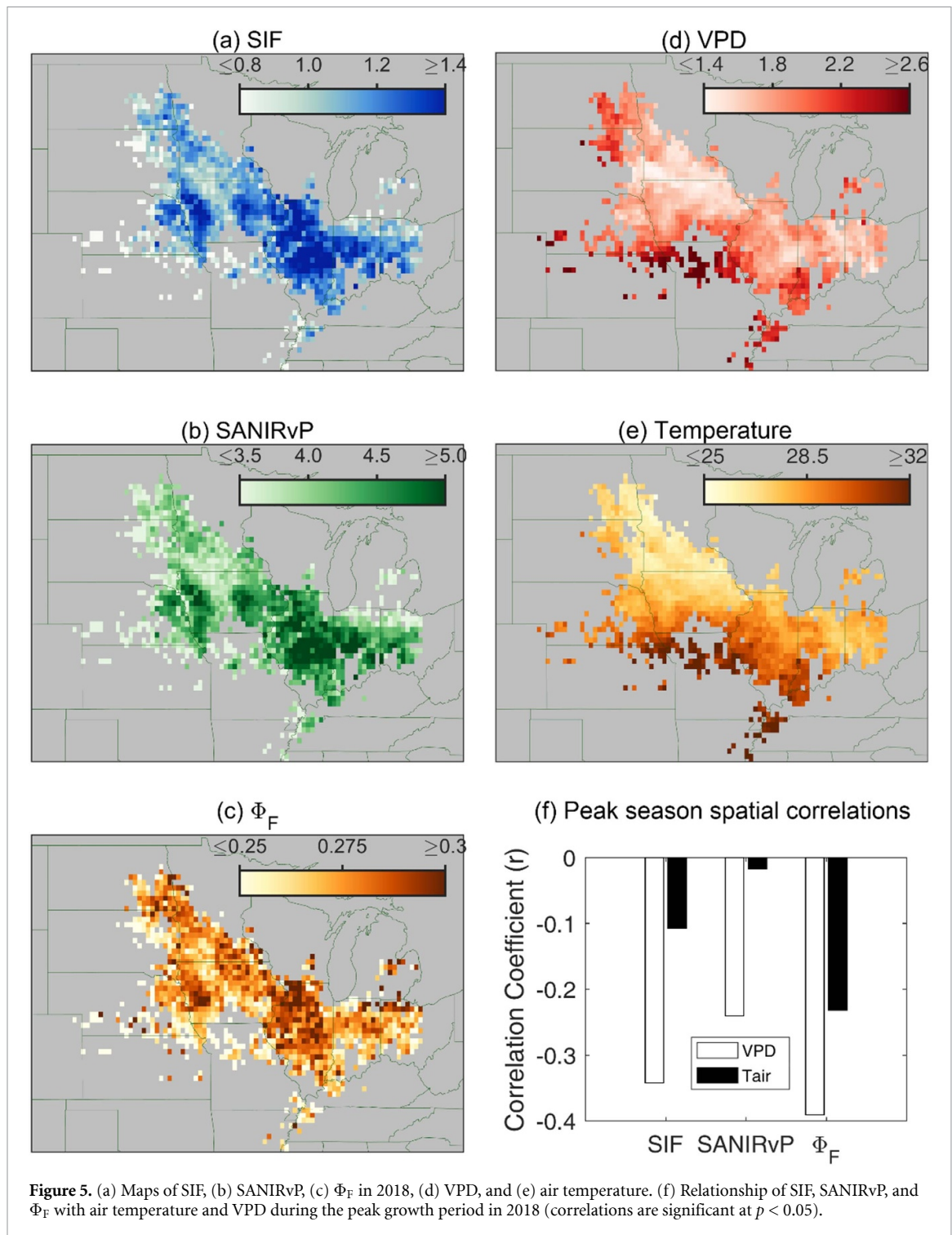


Figure 4. (a) Difference of SIF, NIRvP, and Φ_F between the irrigated and rainfed sites. Φ_F was compared to canopy scale stomatal conductance (G_s) to evaluate its link to plant physiology in both irrigated and rainfed sites (b).

deficit. The comparison between G_s and Φ_F showed a positive linear relationship only in the rainfed site (figure 4(b)). The discovered positive linear relationship between G_s and Φ_F indicated that the observed

Φ_F difference resulted from the physiological stress by water deficit in the rainfed site.

Third, we analyzed the regional-scale data, i.e. TROPOMI SIF, MODIS-based SANIRvP, and



SIF-derived Φ_F . All three variables negatively responded to VPD, and Φ_F showed a greater response to VPD than SANIRvP and SIF (figure 5(d)). For air temperature, the three variables showed a similar pattern with weaker responses than to VPD (figure 5(d)). Only SIF and Φ_F showed a negative response to air temperature, and again, Φ_F showed greater sensitivity than SIF. Considering the findings of the two ground-based sensing datasets, the

relationship of satellite-derived Φ_F with air temperature and VPD suggested that Φ_F variation could be indicative of plant physiological responses. The correlation between SIF and environmental variables showed that SIF may capture plant responses in terms of both canopy structure and plant physiology, but Φ_F separately quantified physiological signals and showed its strength for stress detection through greater sensitivity than SIF.

4. Discussion

4.1. Plant physiological signals, Φ_F , explained a significant portion of SIF variability under different environmental conditions

We first showed a high correlation between SIF and (SA)NIRvP (figure 1), which is consistent with the dominant role of structural information in explaining SIF from previous studies, e.g. SIF was highly correlated with APAR (Miao *et al* 2018, 2020, Yang *et al*, 2018a) and NIRvP (Baldocchi *et al* 2020, Dechant *et al* 2020). The agreement between SIF and NIRvP was predictable considering the pronounced importance of diurnal and seasonal variation of radiation and seasonality of canopy development in SIF. The relative importance of (SA)NIRvP and Φ_F in this study, however, further showed that data preprocessing that controlled temporal variation in radiation and canopy structure amplified Φ_F signals and allowed for investigating Φ_F and plant physiological responses. With all data included, the relative importance of Φ_F was no greater than 20% (5%, 20%, and 0% for the plot-scale, field-scale, and regional-scale datasets, respectively). The highest importance found in the field-scale dataset could be due to the water deficit-induced physiological variability. Meanwhile, the plot-scale dataset showed smaller importance of Φ_F although it also included a large physiological variability due to the warming treatments. The different results of the plot-scale and field-scale datasets might be the coupling of NIRvP and Φ_F . In the plot-scale dataset, the continuity of the warming treatments affected both canopy structure and plant physiology whereas the field-scale dataset showed decoupling of NIRvP and Φ_F (figure 4(a)). After the data preprocessing, the importance of Φ_F increased to 17%–31% in the three datasets (figure 2). Specifically, the importance of Φ_F was greater in the plot-scale and the field-scale datasets than the regional-scale dataset (28%, 31%, and 17%, respectively for the plot-scale, field-scale, and regional-scale dataset). A probable reason is stress factors included in the two ground-based datasets (i.e. high-temperature stress and water deficit stress in the plot-scale and field-scale data, respectively).

4.2. SIF-derived physiological signals indicate and quantify plant physiological impacts of high-temperature and high-VPD stress

We found from the three datasets that the quantified Φ_F contribution to the SIF variation after the data preprocessing was relevant to plant physiological responses. Chlorophyll fluorescence measurements including SIF have long been used to test high-temperature and water stress impacts at the canopy scale (Ač *et al* 2015). However, SIF-derived Φ_F has been only recently evaluated, and in the majority of the previous canopy-scale studies, a lack of explicit consideration of canopy structural impact might

have influenced the interpretations of SIF or SIF yield (i.e. SIF divided by APAR). The data of this study showed that SIF-derived Φ_F allowed for quantifying plant physiological variation and contributed to quantifying plant physiological responses under stress conditions.

Our plot-scale data from the canopy warming experiment revealed that NIRvP indicated a non-physiological impact, and SIF-derived Φ_F was indicative of physiological stress with even greater sensitivity than SIF (figure 5(a)), which is consistent with our expectations based on the theory behind the Φ_F derivation. Meanwhile, the field-scale data showed a positive linear relationship between G_s and Φ_F , which is consistent with a leaf-level finding (Flexas *et al* 2002). Even the irrigated site also showed positive linearity between G_s and Φ_F , which suggests not only soil moisture but also VPD regulated crop physiology (Kimm *et al* 2020a). A recent study, on the other hand, reported asymmetry between Φ_F and G_s (and photochemical quantum yield, Φ_p) responses, which disagrees with our finding (Magney *et al* 2020, Marrs *et al* 2020). However, the asymmetry was found under artificial treatments, i.e. abscisic acid application and pressure cuff-induced xylem embolism, while our result was based on less artificial abiotic stress impacts, and target plants' stress coping mechanism might have differed under artificial treatments.

The relationship between G_s and Φ_F of our analysis suggests that Φ_F is indicative of plant physiological responses because, under the water deficit conditions of our measurements, G_s behavior suggests physiological stress and further, G_s could be mechanistically connected and synchronized with Φ_p . The relation between Φ_p and G_s might be partially explained by mechanisms related to photosynthetic processes. First, there have been investigations on the direct connection between stomatal behavior and photosynthetic electron transfer chain (Sharkey and Raschke 1981, Messinger *et al* 2006, Busch 2014, Głowacka *et al* 2018). The connection between the two components has not been fully understood, but changes in light, i.e. different spectral intensity or modulations in photosystem II, were found to induce stomatal behavioral changes suggesting a direct connection. Second, optimality theory may explain the link between stomatal behavior and light reaction. Stomatal behavior was often understood from a perspective of optimization between carbon gain and water loss (Katul *et al* 2012), and photosynthetic processes were also seen from an optimality perspective utilizing the balance between rubisco carbon fixation and photosynthetic electron transfer rate (Jiang *et al* 2020b). A rate of photosynthesis involves multiple processes including stomatal behavior, and to optimize resource and energy use, plants are expected to balance between the processes resulting in the linearity between G_s and Φ_p .

The SIF-derived Φ_F application also showed the potential with the satellite data analysis and supported the large-scale applicability of Φ_F for SIF-based physiological investigations. Existing studies of satellite-based SIF have found that SIF showed stronger and earlier plant responses to droughts and heat stress than conventional vegetation indices (Sun *et al* 2015, Song *et al* 2018, Li *et al* 2020a). However, what the SIF responses actually suggested remained unclear, e.g. how much of SIF responses were due to the physiological responses or non-physiological variability. Our analysis showed that SIF responses to temperature and VPD were attributed more to Φ_F than SANIRvP, indicating physiological stress than canopy structural depressions. Especially, temperature impact on SIF was largely attributed to Φ_F while almost no response was found in SANIRvP (figure 5(f)), and we found greater sensitivity of Φ_F to climate variables than SIF. The aforementioned relationship of Φ_F with temperature and VPD showed that, despite the large uncertainty, the derived Φ_F suggested plant physiological responses. Its sensitivity to climate variables indicates Φ_F could be more useful than SIF in detecting physiological stresses possibly because Φ_F is unassociated with canopy structural variation, unlike SIF.

4.3. Implications of using Φ_F for ecosystem stress detection

In this study, we quantified SIF-derived Φ_F and demonstrated its capability for physiological investigations in crops. Our results addressed the unique contribution of SIF to remote sensing of crops and showed the potential of SIF for large-scale crop stress quantification. Previous crop SIF studies, however, reported that physiological signals may have a marginal contribution to SIF variations (Miao *et al* 2018, Yang *et al* 2018a, Dechant *et al* 2020), and particularly, studies that investigated SIF-derived Φ_F found the physiological signal relatively constant throughout their datasets (Dechant *et al* 2020, Liu *et al* 2020). We speculate that the different findings about Φ_F were due to two major aspects, i.e. if physiological stresses existed and how tightly physiological stress was coupled with canopy structural variation. First, crop physiological stress tends to be well managed through agricultural management practices such as irrigation and fertilization application (Peng *et al* 2020), and previous crop SIF studies observed crops without stress, and therefore, observed no clear signals of physiological variation. This study, on the other hand, included data of crops with and without high-temperature or high-VPD conditions, and by comparing their difference, we captured strong physiological down-regulation of crop productivity. Second, crop physiological status is largely coupled with canopy structure, and crop productivity largely depends on canopy structure (Wu *et al* 2019, Liu *et al* 2020). The opposite case, for example, is

evergreen ecosystems where canopy structural variation and physiological status are largely decoupled and SIF can quantify physiological variations better than in other ecosystems (Walther *et al* 2016, Magney *et al* 2019, Kim *et al* 2021). In this study, we processed the data constraining variations in radiation and canopy structure to decouple structure and physiology, which allowed the extraction of signals that are related to physiological variations.

5. Conclusion

In this study, we quantified the SIF-derived physiological signal, Φ_F , and investigated whether Φ_F signal quantifies crop physiological responses and contributes to understanding crop responses to environmental stresses. We analyzed three SIF datasets at different spatial scales and platforms, and disaggregation of SIF showed that $\sim 31\%$ of SIF variation was attributable to Φ_F , which was theoretically relevant to plant physiological responses. We further analyzed and demonstrated that Φ_F signals suggested crop physiological responses to high-temperature and water deficit stresses with greater sensitivity to plant responses compared to SIF. The findings were from plot-scale, field-scale, and regional-scale datasets and showed the scalability of Φ_F application for physiological investigations. This study highlights the unique contribution of SIF to remote sensing of vegetation physiology by utilizing Φ_F and emphasizes the potential of Φ_F in understanding plant physiology responses to different environmental conditions as well as the stress-coping mechanisms of plants.

Data availability statement

The data that support the findings of this study are available upon reasonable request from the authors.

Acknowledgments

Guan, Kimm, Ainsworth, and Bernacchi acknowledge financial support from the U.S. Department of Agriculture National Institute of Food and Agriculture Project (20176701326253) titled 'Parsing Multiple Mechanisms of High Temperature Impacts on Soybean Yield Combining Infrared Heating Experiments and Process Based Modeling'. Guan and Kimm acknowledge funding from the National Aeronautics and Space Administration (NASA), Carbon Monitoring System Award (80NSSC18K0170) and Carbon Cycle Science (NNX17AE14G). Guan and Kimm also acknowledge fellowship support from the Illinois Water Resources Center (IWRC) affiliated to the U.S. Geological Survey (USGS) and Block Grant fellowship support from the department of Natural Resources and Environmental Sciences at the University of Illinois Urbana-Champaign. Suyker acknowledges the AmeriFlux Management Project

funding of this core site provided by the U.S. Department of Energy's Office of Science under Contract No. DE-AC02-05CH11231 and partially supported by the Nebraska Agricultural Experiment Station with funding from the Hatch Act (Accession Number 1020768) through the USDA National Institute of Food and Agriculture.

ORCID iDs

Hyungsuk Kimm  <https://orcid.org/0000-0001-8189-0874>
 Kaiyu Guan  <https://orcid.org/0000-0002-3499-6382>
 Chongya Jiang  <https://orcid.org/0000-0002-1660-7320>
 Guofang Miao  <https://orcid.org/0000-0001-5532-932X>
 Genghong Wu  <https://orcid.org/0000-0002-6227-6390>
 Andrew E Suyker  <https://orcid.org/0000-0002-4394-1607>
 Elizabeth A Ainsworth  <https://orcid.org/0000-0002-3199-8999>
 Carl J Bernacchi  <https://orcid.org/0000-0002-2397-425X>
 Christopher M Montes  <https://orcid.org/0000-0002-7295-3092>
 Joseph A Berry  <https://orcid.org/0000-0002-5849-6438>
 Xi Yang  <https://orcid.org/0000-0002-5095-6735>
 Christian Frankenberg  <https://orcid.org/0000-0002-0546-5857>
 Min Chen  <https://orcid.org/0000-0001-6311-7124>
 Philipp Köhler  <https://orcid.org/0000-0002-7820-1318>

References

- Ač A, Malenovský Z, Olejníčková J, Gallé A, Rascher U and Mohammed G 2015 Meta-analysis assessing potential of steady-state chlorophyll fluorescence for remote sensing detection of plant water, temperature and nitrogen stress *Remote Sens. Environ.* **168** 420–36
- Badgley G, Anderegg L D L, Berry J A and Field C B 2019 Terrestrial gross primary production: using NIR V to scale from site to globe *Glob. Change Biol.* **25** 1–10
- Badgley G, Field C B and Berry J A 2017 Canopy near-infrared reflectance and terrestrial photosynthesis *Sci. Adv.* **3** e1602244
- Baldocchi D D *et al* 2020 Outgoing near-infrared radiation from vegetation scales with canopy photosynthesis across a spectrum of function, structure, physiological capacity, and weather *J. Geophys. Res. Biogeosci.* **125** e2019JG005534
- Busch F A 2014 Opinion: the red-light response of stomatal movement is sensed by the redox state of the photosynthetic electron transport chain *Photosynth. Res.* **119** 131–40
- Cai Y *et al* 2019 Integrating satellite and climate data to predict wheat yield in Australia using machine learning approaches *Agric. For. Meteorol.* **274** 144–59
- Dechant B *et al* 2020 Canopy structure explains the relationship between photosynthesis and sun-induced chlorophyll fluorescence in crops *Remote Sens. Environ.* **241** 111733
- Dechant B *et al* 2022 NIRvP: a robust structural proxy for sun-induced chlorophyll fluorescence and photosynthesis across scales *Remote Sens. Environ.* **268** 112763
- Erdle K, Mistele B and Schmidhalter U 2013 Spectral high-throughput assessments of phenotypic differences in biomass and nitrogen partitioning during grain filling of wheat under high yielding Western European conditions *Field Crops Res.* **141** 16–26
- Fleta-Soriano E and Munné-Bosch S 2016 Stress memory and the inevitable effects of drought: a physiological perspective *Front. Plant Sci.* **7** 143
- Flexas J, Escalona J M, Evain S, Gulías J, Moya I, Osmond C B and Medrano H 2002 Steady-state chlorophyll fluorescence (Fs) measurements as a tool to follow variations of net CO₂ assimilation and stomatal conductance during water-stress in C₃ plants *Eur. Sp. Agency (Special Publ. ESA SP)* pp 26–29
- Gitelson A A, Viña A, Ciganda V, Rundquist D C and Arkebauer T J 2005 Remote estimation of canopy chlorophyll content in crops *Geophys. Res. Lett.* **32** L08403
- Głowacka K, Kromdijk J, Kucera K, Xie J, Cavanagh A P, Leonelli L, Leakey A D B, Ort D R, Niyogi K K and Long S P 2018 Photosystem II subunit S overexpression increases the efficiency of water use in a field-grown crop *Nat. Commun.* **9** 868
- Guan K, Berry J A, Zhang Y, Joiner J, Guanter L, Badgley G and Lobell D B 2016 Improving the monitoring of crop productivity using spaceborne solar-induced fluorescence *Glob. Change Biol.* **22** 716–26
- Guan K, Wu J, Kimball J S, Anderson M C, Frolking S, Li B, Hain C R and Lobell D B 2017 The shared and unique values of optical, fluorescence, thermal and microwave satellite data for estimating large-scale crop yields *Remote Sens. Environ.* **199** 333–49
- Hatfield J L, Gitelson A A, Schepers J S and Walthall C L 2008 Application of spectral remote sensing for agronomic decisions *Agron. J.* **100** 117–31
- Hatfield J L and Prueger J H 2015 Temperature extremes: effect on plant growth and development *Weather Clim. Extrem.* **10** 4–10
- Helm L T, Shi H, Lerdau M and Yang X 2020 Solar-induced chlorophyll fluorescence and short-term photosynthetic response to drought *Ecol. Appl.* **30** e02101
- Jiang C, Guan K, Wu G, Peng B and Wang S 2020a A daily, 250 m and real-time gross primary productivity product (2000–present) covering the Contiguous United States *Earth Syst. Sci. Data Discuss.* **2020** 1–28
- Jiang C, Ryu Y, Wang H and Keenan T F 2020b An optimality-based model explains seasonal variation in C₃ plant photosynthetic capacity *Glob. Change Biol.* **26** 1354–1013
- Katul G G, Oren R, Manzoni S, Higgins C and Parlange M B 2012 Evapotranspiration: a process driving mass transport and energy exchange in the soil-plant-atmosphere-climate system *Rev. Geophys.* **50** RG3002
- Kim J, Ryu Y, Dechant B, Lee H, Kim H S, Kornfeld A and Berry J A 2021 Solar-induced chlorophyll fluorescence is non-linearly related to canopy photosynthesis in a temperate evergreen needleleaf forest during the fall transition *Remote Sens. Environ.* **258** 112362
- Kimm H *et al* 2020b Deriving high-spatiotemporal-resolution leaf area index for agroecosystems in the U.S. Corn Belt using Planet Labs CubeSat and STAIR fusion data *Remote Sens. Environ.* **239** 111615
- Kimm H *et al* 2021 Quantifying high-temperature stress on soybean canopy photosynthesis: the unique role of sun-induced chlorophyll fluorescence *Glob. Change Biol.* **27** 2403–15
- Kimm H, Guan K, Gentine P, Wu J, Bernacchi C J, Sulman B N, Griffis T J and Lin C 2020a Redefining droughts for the U.S. Corn Belt: the dominant role of atmospheric vapor pressure deficit over soil moisture in regulating stomatal behavior of maize and soybean *Agric. For. Meteorol.* **287** 107930

- Köhler P, Frankenberg C, Magney T S, Guanter L, Joiner J and Landgraf J 2018 Global retrievals of solar-induced chlorophyll fluorescence with TROPOMI: first results and intersensor comparison to OCO-2 *Geophys. Res. Lett.* **45** 10.456–10.463
- Li X, Xiao J, Kimball J S, Reichle R H, Scott R L, Litvak M E, Bohrer G and Frankenberg C 2020a Synergistic use of SMAP and OCO-2 data in assessing the responses of ecosystem productivity to the 2018 U.S. drought *Remote Sens. Environ.* **251** 112062
- Li Z, Zhang Q, Li J, Yang X, Wu Y, Zhang Z, Wang S, Wang H and Zhang Y 2020b Solar-induced chlorophyll fluorescence and its link to canopy photosynthesis in maize from continuous ground measurements *Remote Sens. Environ.* **236** 111420
- Liu L, Guan L and Liu X 2017 Directly estimating diurnal changes in GPP for C3 and C4 crops using far-red sun-induced chlorophyll fluorescence *Agric. For. Meteorol.* **232** 1–9
- Liu L, Liu X, Chen J, Du S, Ma Y, Qian X, Chen S and Peng D 2020 Estimating maize GPP using near-infrared radiance of vegetation *Sci. Remote Sens.* **2** 100009
- Lobell D B, Thau D, Seifert C, Engle E and Little B 2015 A scalable satellite-based crop yield mapper *Remote Sens. Environ.* **164** 324–33
- Magney T S et al 2019 Mechanistic evidence for tracking the seasonality of photosynthesis with solar-induced fluorescence *Proc. Natl Acad. Sci.* **116** 201900278
- Magney T S, Barnes M L and Yang X 2020 On the covariation of chlorophyll fluorescence and photosynthesis across scales *Geophys. Res. Lett.* **47** e2020GL091098
- Marrs J K, Reblin J S, Logan B A, Allen D W, Reinmann A B, Bombard D M, Tabachnik D and Hutryra L R 2020 Solar-induced fluorescence does not track photosynthetic carbon assimilation following induced stomatal closure *Geophys. Res. Lett.* **47** e2020GL087956
- Messinger S M, Buckley T N and Mott K A 2006 Evidence for involvement of photosynthetic processes in the stomatal response to CO₂ *Plant Physiol.* **140** 771–8
- Miao G et al 2018 Sun-induced chlorophyll fluorescence, photosynthesis, and light use efficiency of a soybean field from seasonally continuous measurements *J. Geophys. Res. Biogeosci.* **123** 610–23
- Miao G et al 2020 Varying contributions of drivers to the relationship between canopy photosynthesis and far-red sun-induced fluorescence for two maize sites at different temporal scales *J. Geophys. Res. Biogeosci.* **125** e2019JG005051
- Peng B et al 2020 Towards a multiscale crop modelling framework for climate change adaptation assessment *Nat. Plants* **6** 338–48
- Porcar-Castell A, Tyystjärvi E, Atherton J, van der Tol C, Flexas J, Pfündel E E, Moreno J, Frankenberg C and Berry J A 2014 Linking chlorophyll a fluorescence to photosynthesis for remote sensing applications: mechanisms and challenges *J. Exp. Bot.* **65** 4065–95
- Sharkey T D and Raschke K 1981 Effect of light quality on stomatal opening in leaves of *Xanthium strumarium* L *Plant Physiol.* **68** 1170–4
- Song L, Guanter L, Guan K, You L, Huete A, Ju W and Zhang Y 2018 Satellite sun-induced chlorophyll fluorescence detects early response of winter wheat to heat stress in the Indian Indo-Gangetic Plains *Glob. Change Biol.* **24** 4023–37
- Sun Y, Fu R, Dickinson R, Joiner J, Frankenberg C, Gu L, Xia Y and Fernando N 2015 Drought onset mechanisms revealed by satellite solar-induced chlorophyll fluorescence: insights from two contrasting extreme events *J. Geophys. Res. Biogeosci.* **120** 2427–40
- van der Tol C, Berry J A, Campbell P K E and Rascher U 2014 Models of fluorescence and photosynthesis for interpreting measurements of solar-induced chlorophyll fluorescence *J. Geophys. Res. Biogeosci.* **119** 2312–27
- Viña A, Gitelson A A, Nguy-Robertson A L and Peng Y 2011 Comparison of different vegetation indices for the remote assessment of green leaf area index of crops *Remote Sens. Environ.* **115** 3468–78
- Walther S, Voigt M, Gonsamo A, Zhang Y, Khler P, Jung M, Varlagin A and Guanter L 2016 Satellite chlorophyll fluorescence measurements reveal large-scale decoupling of photosynthesis and greenness dynamics in boreal evergreen forests *Glob. Change Biol.* **22** 2979–96
- Wu G et al 2019 Radiance-based NIRv as a proxy for GPP of corn and soybean *Environ. Res. Lett.* **15** 034009
- Xie Y, Lark T J, Brown J F and Gibbs H K 2019 Mapping irrigated cropland extent across the conterminous United States at 30 m resolution using a semi-automatic training approach on Google Earth Engine *ISPRS J. Photogramm. Remote Sens.* **155** 136–49
- Yang K et al 2018a Sun-induced chlorophyll fluorescence is more strongly related to absorbed light than to photosynthesis at half-hourly resolution in a rice paddy *Remote Sens. Environ.* **216** 658–73
- Yang X, Shi H, Stovall A, Guan K, Miao G, Zhang Y, Zhang Y, Xiao X, Ryu Y and Lee J E 2018b FluoSpc 2—an automated field spectroscopy system to monitor canopy solar-induced fluorescence *Sensors* **18** 2063
- Zeng Y et al 2020 A radiative transfer model for solar induced fluorescence using spectral invariants theory *Remote Sens. Environ.* **240** 111678
- Zeng Y, Badgley G, Dechant B, Ryu Y, Chen M and Berry J A 2019 A practical approach for estimating the escape ratio of near-infrared solar-induced chlorophyll fluorescence *Remote Sens. Environ.* **232** 111209
- Zhang J et al 2021 Challenges and opportunities in precision irrigation decision-support systems for center pivots *Environ. Res. Lett.* **16** 053003